MINAR International Journal of Applied Sciences and Technology
(Minar Journal)

STUDY OF THE STRUCTURAL, OPTICAL AND ELECTRICAL PROPERTIES OF PBO:CDO THIN FILM AT ROOM TEMPERATURE

Anas A. ABDULLAH
University of Tikrit ,, Iraq

Guson H. MOHAMMED
University of Baghdad, Iraq

Sabri J. MOHAMMED
University of Tikrit , Iraq

Article Information

Research Article

November 2019

Volume: 1

Issue: 1

p. 20-31

Article History

Received
02/10/2019

Accepted
15/10/2019

Available online
15/11/2019

Plagiarism

This article has been scanned by **iThenticat**

No plagiarism detecte

Abstract:

In this research, pulse laser deposition Nd:YAG has 1064 nm wavelength, with a number of 400 shoots, was used to produce (PbO:CdO) thin films with different ratio (0.1, 0.3 , 0.5, 0.7 and 0.9) atom at room temperature under vacuum. The films were examined by UV-Visible spectroscopy ,X-ray diffraction and Atomic force microscope to study the effect of film ratio on it properties. It was found that the absorption decrease with increasing CdO ratio from 3.5 to 0.7 at 600 nm, while the energy gap increase from 2.6 to 2.9 eV with it. Electrical properties show enhance the films conductivity with increasing CdO ratio and convert from P-type to n-type at 0.5 PbO:CdO thin films ratio.

Keywords: PbO:CdO Thin Film, Pulse laser deposition, XRD

Introduction:

A thin film is the geometrical description of material having one of its dimension about one micron or less. The thin films have unique properties significantly different from the bulk materials as a result of their physical dimensions, geometry and non equilibrium microstructure[1]. Pulsed Laser Deposition (PLD) is a thin film deposition technique based on the interaction between a high-power pulsed laser beam and a target of the material we want to deposit in thin film configuration. The laser beam is focused on the target surface and, if the energy density is higher than an energy threshold, the material is ablated from the target surface [2].

Lead Oxide (PbO), an important industrial material, has been widely applied in gas sensors, pigments and paints . PbO has two polymorphic forms and a wide band gap: red α-PbO, stable at low temperature, and yellow β-PbO, stable at high temperature[3]. Nanoparticles have attracted great interest in recent years because of their unique chemical and physical properties, which are different from those of either the bulk materials or single atoms. In recent years, researchers have focused on cadmium oxide (CdO) due to its applications, specifically in the field of optoelectronic devices such as solar cells , photo transistors and diodes , transparent electrodes , gas sensors , etc[4].

X- ray diffraction used to characterize obtained films crystallinety. The d_{hkl} spacing between crystals planes can deduced by X-ray diffraction using Bragg's law [5].

$$n\lambda = 2\, d_{hkl} \sin\theta \quad \ldots\ldots\ldots\ldots\ldots\ldots\ldots(1)$$

where θ is diffraction angle and λ is the used XRD wavelength.

Scherrer equation formula used to calculate crystalline size utilize the peaks broadening [6].

$$G.S = \frac{0.9\,\lambda}{FWHM\,.\cos(\theta)} \quad \ldots\ldots\ldots\ldots\ldots\ldots\ldots(2)$$

Where λ is the x-ray wavelength for k_α transition from Cu target (1.5406 Å), FWHM is full width at half maximum and θ is the angle of diffraction.

The AFM is capable of measuring nanometer scale images of surfaces as well as measuring three dimensional images of surfaces and studying the topography[7].

The fundamental absorption is the most important absorption process which involves the transition of electrons from the valence to the conduction band, which

show itself by a rapid elevation in the absorption and this can be used to determine the energy gap of the semiconductor [8]. Energy gap can be calculated from the following equation[9]

$$\alpha h\nu = B\left(h\nu - E_g\right)^{1/2} \quad \text{.....(3)}$$

Semiconductor thin films conductivity depend on its temperature as described by the relation

$$\sigma = \sigma_o \exp(-E_a/k_B T) \quad \text{..... (4)}$$

Where E_a is the activation energy, which can be calculated from the plot of lnσ versus 1000/T according to equation: Where σ_o is the minimum electrical conductivity at 0K, T is the temperature and k_B are the Boltzmann's constant [10].

Experimental Part

Lead oxide (PbO) with purity (99.98 %) powder by BDH chemical limited, England Company and Cadmium oxide (CdO), with purity (99.9 %) by VIO SOJUZCHIMEXPORT USSR, were used in this thesis. Bulk PbO:CdO samples have been prepared using of the of two material by Grinded and mixed together at a different concentration of (x = 0.1 , 0.3 , 0.5 , 0.7 , 0.9) atom % for (10minute), then pressed into pellets with (1.2 cm) diameter using hydraulic piston type (SPECAC), under the pressure of 6 tons/cm^2 for 10 minutes, as shown in Fig. (1). The pellets are sintered in air to temperature (873 K) for 1 hours then cooled to room temperature.

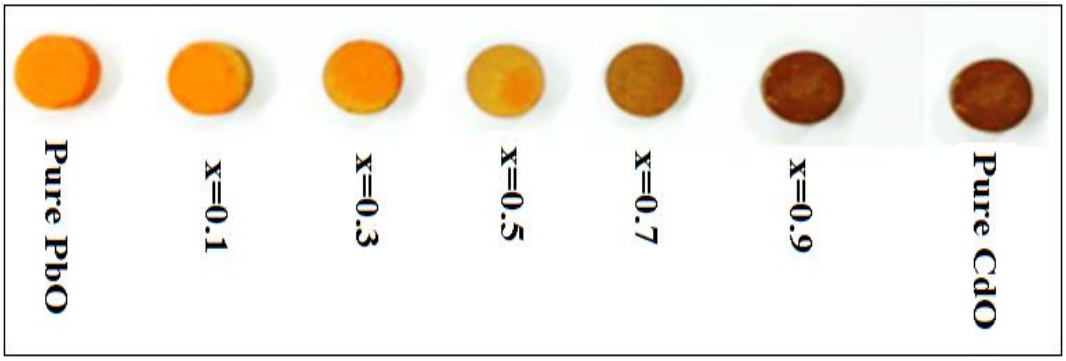

Fig. (1):The used pellets with different concentration

The pure and composite thin films were prepared by pulsed laser deposition technique (PLD) λ = 1064 nm with 500 mJ peak power inside a vacuum chamber, at 10^{-2} mbar pressure, using double stage rotary pump. The films were deposited on glass substrates at RT. The schematic of laser deposition set-up was shown in Fig.(2). The Nd:YAG was focused on target through the glass chamber making an angle of 45° with the target surface. The substrate is placed above the target at 3 cm distance.

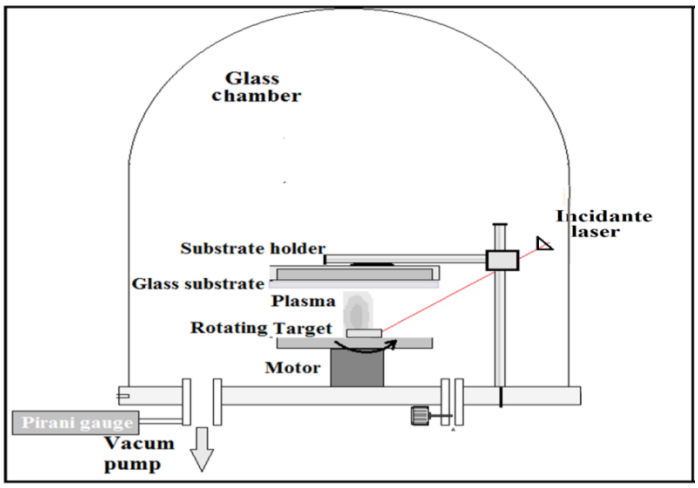

Fig. (2) Schematic for pulse laser deposition set up.

The produced films were examined by X-ray diffraction (XRD) , AFM (AA3000 Scanning Probe Microscope SPM. Angstrom Ad-Vance Inc, tip NSC35/AIBS) and UV-visible absorption to study the effect of ratio on thin films structural and their optical properties.

Results and Discussion

Fig. (3) shows the X- ray diffraction patterns for PbO, CdO and their composite with different ratio, deposited by pulse laser deposition on glass substrate for as deposited samples . The pure PbO sample has many peaks corresponding to three phase, Tetragonal PbO, Orthorhombic PbO and Tetragonal Pb_3O_4, with preferred orientation along (011) Tetragonal PbO. There are some peaks correspond to Hexagonal Cd phase at the (0.3 ,0.5) ratio, also new peaks corresponding to Cubic $CdPbO_3$ phase at the (0.7) ratio. These patterns shows that increase the CdO ratio cause to appear of new peaks corresponding to CdO and, while the decreasing in PbO peaks intensities till finished at the (0.9) ratio and only CdO peaks appeared. These peak increased with increasing ratio indicated on enhance the film crystallinty, and it is found that the crystalline size for PbO particles decrease, while for CdO increase with increasing the composite ratio. The pure CdO sample shows very broad peaks which indicate on formation of nanomaterial.

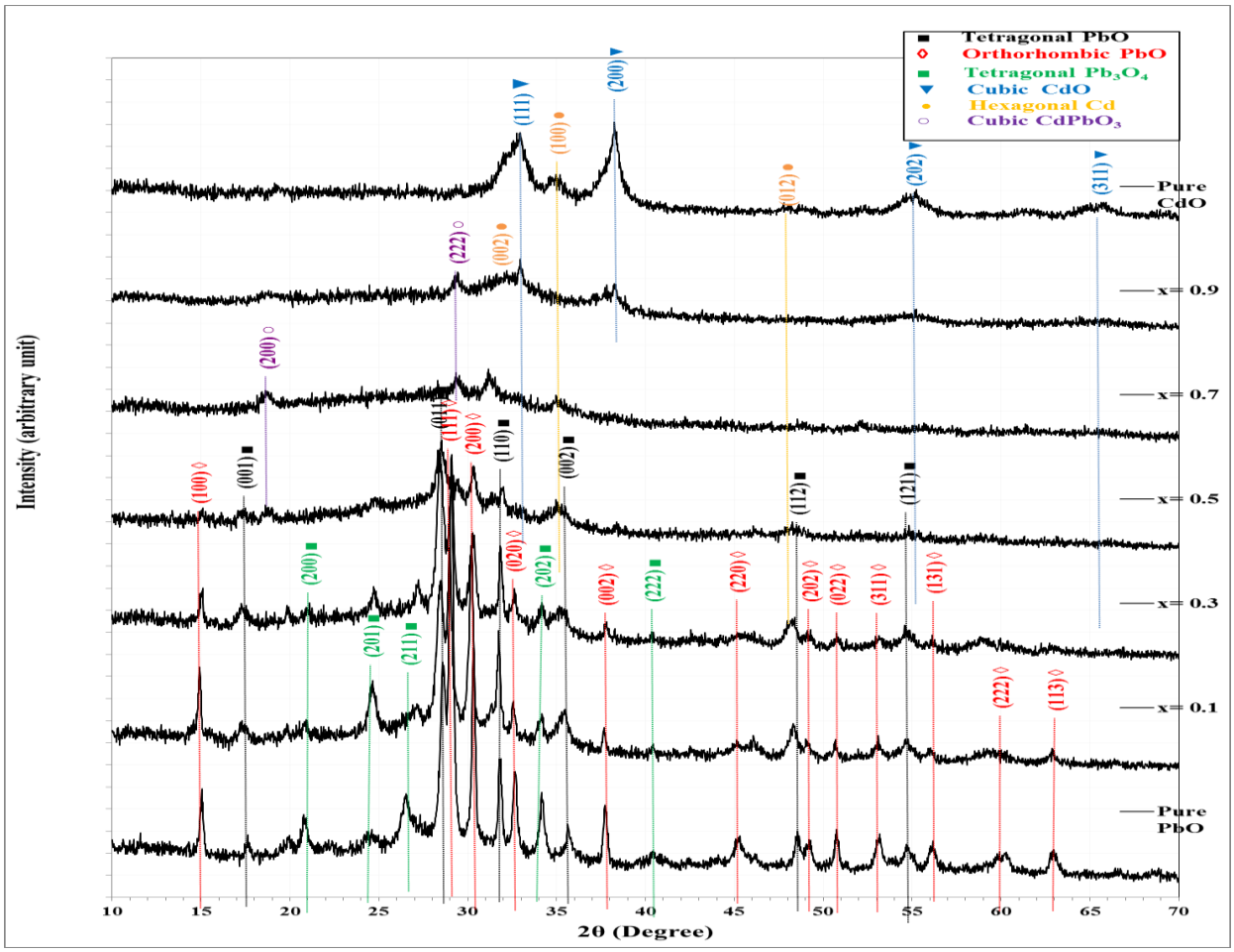

Fig. 3 : XRD patterns for $(PbO)_{1-x}(CdO)_x$ thin films at room temperature.

Table (1): X-ray patterns parameters for $(PbO)_{1-x}(CdO)_x$ thin films

sample	2θ (Deg.)	FWHM (Deg.)	d_{hkl} Exp.(Å)	G.S (nm)	d_{hkl} Std.(Å)	Phase	hkl	card No.
Pure PbO	15.0266	0.2793	5.8911	28.7	5.8931	Orth. PbO	(100)	96-900-7711
	17.6197	0.3989	5.0295	20.2	5.0435	Tet. PbO	(001)	96-901-2703
	20.7713	0.4388	4.2730	18.4	4.4055	Tet. Pb_3O_4	(200)	96-901-2125
	28.5904	0.3590	3.1197	22.8	3.127	Tet. PbO	(011)	96-901-2703
	28.9894	0.3590	3.0776	22.9	3.0680	Orth. PbO	(111)	96-900-7711
	30.3059	0.2792	2.9469	29.5	2.9465	Orth. PbO	(200)	96-900-7711
	31.7819	0.2394	2.8133	34.5	2.8181	Tet. PbO	(110)	96-901-2703
	34.1755	0.4388	2.6215	18.9	2.6317	Tet. Pb_3O_4	(202)	96-901-2125
	35.6516	0.4389	2.5163	19.0	2.5217	Tet. PbO	(002)	96-901-2703
	37.7261	0.3191	2.3826	26.3	2.3764	Orth. PbO	(002)	96-900-7711
	40.4388	0.5984	2.2288	14.1	2.2593	Tet. Pb_3O_4	(222)	96-901-2125
	45.2660	0.5984	2.0017	14.4	2.0086	Orth. PbO	(220)	96-900-7711
	48.5372	0.3590	1.8741	24.3	1.8792	Tet. PbO	(112)	96-901-2703
	53.2048	0.3990	1.7202	22.3	1.7236	Orth. PbO	(311)	96-900-7711
	54.7606	0.5585	1.6749	16.0	1.6805	Tet. PbO	(121)	96-901-2703
	56.1569	0.5186	1.6366	17.4	1.6404	Orth. PbO	(131)	96-900-7711
	62.9388	0.5186	1.4755	18.0	1.4738	Orth. PbO	(113)	96-900-7711
0.1	14.9069	0.1995	5.9381	40.2	5.8931	Orth. PbO	(100)	96-900-7711
	27.1543	0.6383	3.2813	12.8	3.3783	Tet. Pb_3O_4	(211)	96-901-2125
	28.4707	0.4388	3.1325	18.7	3.127	Tet. PbO	(011)	96-901-2703
	29.0691	0.2792	3.0694	29.4	3.0680	Orth. PbO	(111)	96-900-7711
	31.7420	0.2793	2.8167	29.6	2.8181	Tet. PbO	(110)	96-901-2703
	32.5399	0.3192	2.7495	25.9	2.7452	Orth. PbO	(020)	96-900-7711
	34.1755	0.3590	2.6215	23.2	2.6317	Tet. Pb_3O_4	(202)	96-901-2125
	35.4122	0.6782	2.5328	12.3	2.5217	Tet. PbO	(002)	96-901-2703
	37.6463	0.2394	2.3874	35.1	2.3764	Orth. PbO	(002)	96-900-7711
	40.3989	0.3989	2.2309	21.2	2.2593	Tet. Pb_3O_4	(222)	96-901-2125
	45.1862	0.5984	2.0050	14.4	2.0086	Orth. PbO	(220)	96-900-7711
	48.2979	0.5585	1.8829	15.6	1.8792	Tet. PbO	(112)	96-901-2703
	50.6915	0.3990	1.7994	22.0	1.7967	Orth. PbO	(022)	96-900-7711
	53.1250	0.5186	1.7226	17.1	1.7236	Orth. PbO	(311)	96-900-7711
	54.6809	0.7979	1.6772	11.2	1.6805	Tet. PbO	(121)	96-901-2703
	59.8271	1.3962	1.5446	6.6	1.5340	Orth. PbO	(222)	96-900-7711
	62.8590	0.4787	1.4772	19.4	1.4738	Orth. PbO	(113)	96-900-7711
0.3	17.2606	0.6782	5.1333	11.8	5.0435	Tet. PbO	(001)	96-901-2703
	21.0505	0.5585	4.2169	14.5	4.4055	Tet. Pb_3O_4	(200)	96-901-2125
	24.7207	0.5585	3.5985	14.6	3.6578	Tet. Pb_3O_4	(201)	96-901-2125
	28.3511	0.4787	3.1454	17.1	3.127	Tet. PbO	(011)	96-901-2703
	29.0691	0.2792	3.0694	29.4	3.0680	Orth. PbO	(111)	96-900-7711
	30.3059	0.3989	2.9469	20.6	2.9465	Orth. PbO	(200)	96-900-7711
	31.8218	0.2793	2.8099	29.6	2.8181	Tet. PbO	(110)	96-901-2703
	32.6197	0.3590	2.7429	23.1	2.7452	Orth. PbO	(020)	96-900-7711
	34.2154	0.5585	2.6186	14.9	2.6317	Tet. Pb_3O_4	(202)	96-901-2125
	35.3324	0.8378	2.5383	10.0	2.5217	Tet. PbO	(002)	96-901-2703
	37.8457	0.4787	2.3753	17.5	2.3764	Orth. PbO	(002)	96-900-7711
	40.4388	0.4388	2.2288	19.3	2.2593	Tet. Pb_3O_4	(222)	96-901-2125
	45.3059	1.0771	2.0000	8.0	2.0086	Orth. PbO	(220)	96-900-7711
	48.2580	0.6782	1.8843	12.8	1.8792	Tet. PbO	(112)	96-901-2703
	49.2553	0.5585	1.8485	15.6	1.8498	Orth. PbO	(202)	96-900-7711
	53.2447	0.5186	1.7190	17.1	1.7236	Orth. PbO	(311)	96-900-7711
	54.6410	0.8378	1.6783	10.7	1.6805	Tet. PbO	(121)	96-901-2703
	56.1569	0.7978	1.6366	11.3	1.6404	Orth. PbO	(131)	96-900-7711
0.5	15.1064	0.5586	5.8602	14.3	5.8931	Orth. PbO	(100)	96-900-7711
	17.3005	0.9175	5.1216	8.8	5.0435	Tet. PbO	(001)	96-901-2703
	28.5505	0.5585	3.1239	14.7	3.127	Tet. PbO	(011)	96-901-2703
	30.3457	0.5186	2.9431	15.9	2.9465	Orth. PbO	(200)	96-900-7711
	31.5027	0.8378	2.8376	9.9	2.8181	Tet. PbO	(110)	96-901-2703
	35.0532	1.1569	2.5579	7.2	2.5217	Tet. PbO	(002)	96-901-2703
	48.2979	0.9974	1.8829	8.7	1.8792	Tet. PbO	(112)	96-901-2703
	54.7606	0.6383	1.6749	14.0	1.6805	Tet. PbO	(121)	96-901-2703
0.7	18.6569	0.8776	4.7522	9.2	5.2265	Cub. CdPb	(200)	96-100-1049
	29.3484	0.7580	3.0408	10.8	3.0175	Cub. CdPb	(222)	96-100-1049
	31.1436	0.7181	2.8695	11.5	2.8035	Hex. Cd	(002)	96-101-1004
	35.0532	0.8776	2.5579	9.5	2.5748	Hex. Cd	(100)	96-101-1004
0.9	29.3085	0.7580	3.0448	10.8	3.0175	Cub. CdPb	(222)	96-100-1049
	33.0186	0.5984	2.7107	13.8	2.8035	Hex. Cd	(002)	96-101-1004
	38.2846	0.7580	2.3491	11.1	2.3495	Cub. CdO	(200)	96-101-1004
Pure CdO	32.8590	1.3165	2.7235	6.3	2.7130	Cub. CdO	(111)	96-101-1004
	34.9335	1.1170	2.5664	7.5	2.5748	Hex. Cd	(100)	96-101-1004
	38.3245	1.0771	2.3467	7.8	2.3495	Cub. CdO	(200)	96-101-1004
	47.9787	0.5984	1.8946	14.5	1.8963	Hex. Cd	(012)	96-101-1004
	55.0798	1.1170	1.6660	8.0	1.6613	Cub. CdO	(202)	96-101-1004
	65.4521	0.9974	1.4248	9.5	1.4168	Cub. CdO	(311)	96-101-1004

Fig. (4) shows the AFM images and the granulate accumulation for the composite $(PbO)_{1-x}(CdO)_x$ thin films with different content (x=0, 0.1, 0.3, 0.5, 0.7, 0.9 and 1) at room temperature analyzed by Atomic Force Microscope (AFM). This figure shows a uniformly distributed samples with particle size increase with increasing CdO content. Also it was observed that the surfaces of the films exhibited a certain degree of roughness and the film became rougher as the concentration increases. This result indicates that the growth of larger grains at 0.3 ratio leads to increase in the surface roughness.

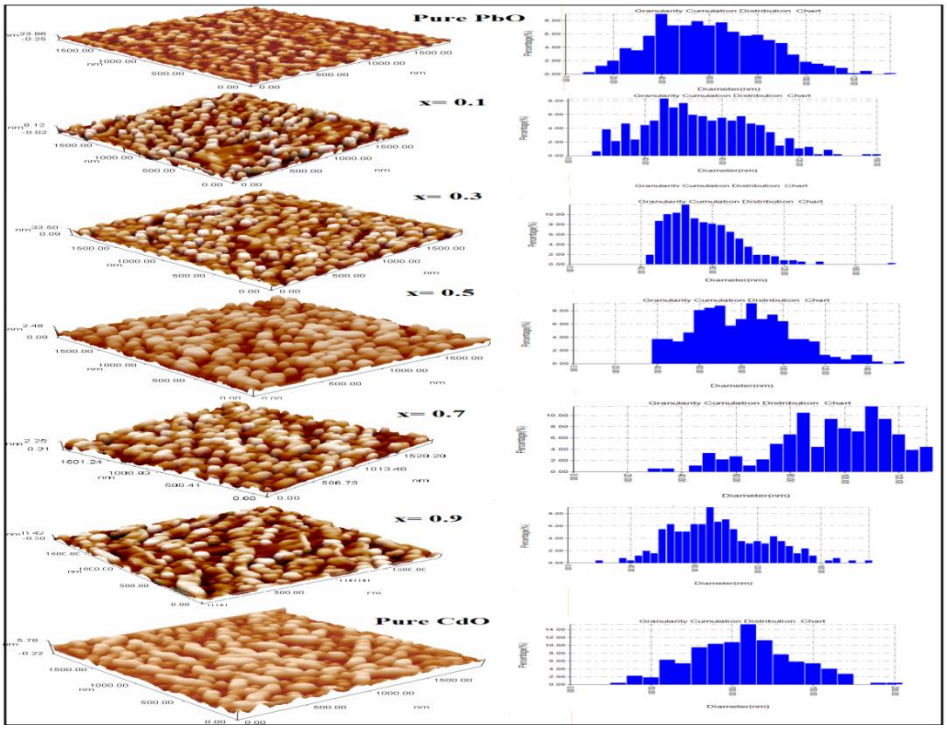

Fig. 4 : Surface morphology of the PbO_{1-x} CdO_x thin films the analyzed by (AFM) before annealing.

Table (2) AFM parameters (Average Diameter, RMS roughness and Peak-peak distance) for $(PbO)_{1-x}(CdO)_x$ thin films before annealing.

Sample	Average Diameter (nm)	RMS roughness (nm)	Peak-peak (nm)
PbO	57.91	2.29	7.75
X=0.1	65.74	2.35	8.14
X=0.3	72.25	8.33	33.4
X=0.5	78.70	0.523	1.83
X=0.7	92.63	0.552	2.04
X=0.9	93.74	3.28	11.7
CdO	101.57	1.11	3.71

Optical transmittance and visual absorption of the spectrums depend on the chemical composition, crystalline structure, material energy gap and morphology of the film surface. The absorbance spectra of the PbO, CdO and there composites thin films, recorded in the wavelength of 300 to 1100 nm, are compared as a function of absorption in the different ratios in Fig.(5) The average absorption varies from 500 to 900 nm where it starts from 2.5 down to 2 for pure PbO sample and the absorption spectrum decreases whenever there is higher the CdO ratio, so in 0.3 and 0.5 ratios the absorption spectrum will be in between 1.76 and 0.8, the absorption decreases more for pure CdO thin film, which may be due to the increase in the percentage of cadmium oxide.

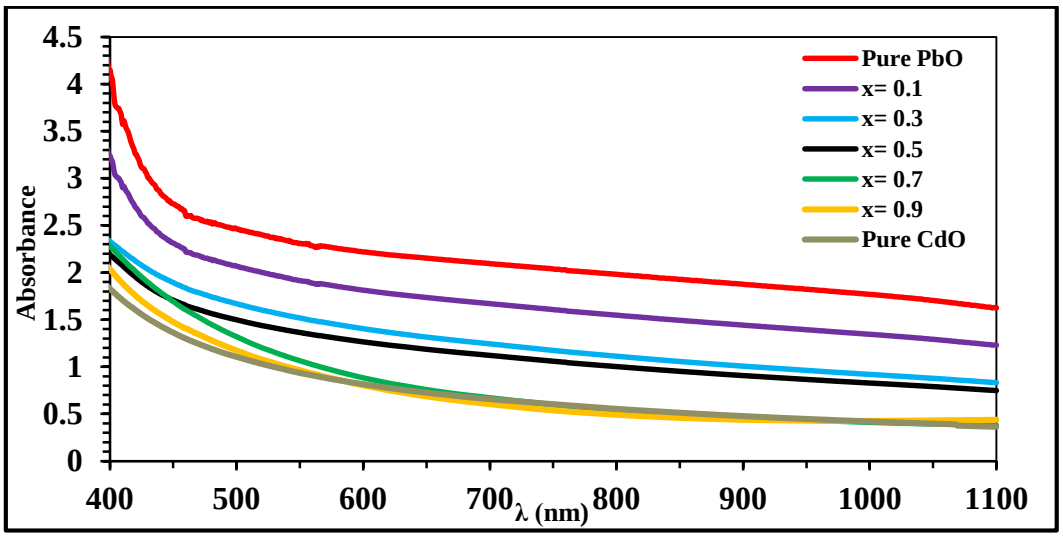

Fig. 5 : Absorption spectra for as deposited PbO_{1-x} CdO_x thin films

The optical energy gap is one of the most important constants in semiconductor physics effect on other physical properties and the field of its applications. In Fig.(6), the optical energy gap values is determined at room temperature. The energy gap values were increased with increasing cadmium oxide content. The owing of increasing the energy gap with increasing CdO content for non-annealed samples as a result of decreasing the crystalline size and forming the nano structures as shown in XRD.

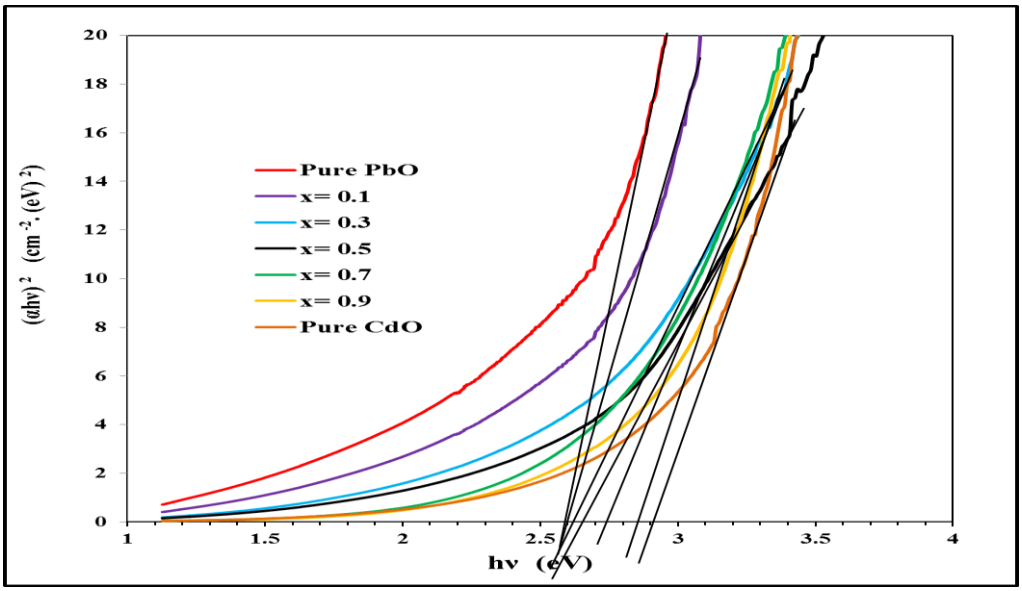

Fig. 6 : energy gap calculation for as deposited PbO_{1-x} CdO_x thin films

Table 3: Transmission, absorption coefficient at 600 nm wavelength and energy gap for at room temperature PbO_{1-x} CdO_x thin films

Sample	T%	α (cm^{-1})	Eg (eV)
PbO	0.60	102207	2.60
x=0.1	1.54	83415	2.60
x=0.3	3.95	64622	2.65
x=0.5	5.45	58197	2.67
x=0.7	13.12	40620	2.75
x=0.9	15.73	36995	2.85
CdO	15.32	37520	2.90

Figs.(7) show the logarithmic change of the electrical conductivity (lnσ) with the inverse absolute temperature (1000 / T) of the PbO and CdO and their composite thin films prepared by pulsed laser deposition at room temperature a. It is clear that there are two types of activation energies E_{a1} and E_{a2} the values of activation energies are calculated using the relationship (4), by determine a slope of tangent to logarithm conductivity ln (σ) as a function of the inverse absolute temperature (1000 / T) multiplied by the Boltzmann constant (k_B) in units (eV).

Table (4) shows the values of activation energies and increased electrical conductivity with increasing cadmium oxide ratio.

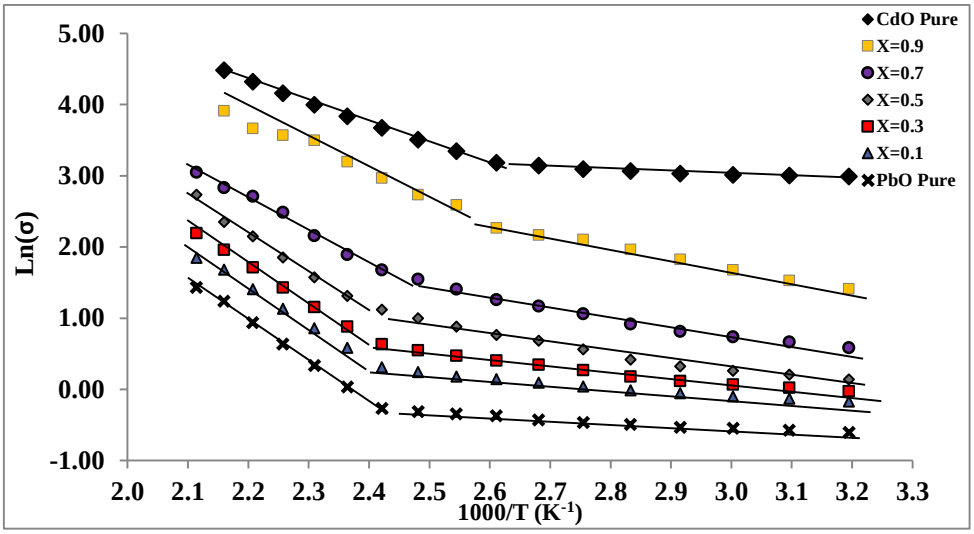

Fig. 7: variation of DC conductivity with 1000/T for as deposited PbO_{1-x} CdO_x thin films

Table 4 : activation energies and their ranges for as deposited PbO_{1-x} CdO_x thin films

Sample	E_{a1} (eV)	Range (K)	E_{a2} (eV)	Range (K)	σ_{RT} ($\Omega^{-1}.cm^{-1}$)
PbO	0.032	313-383	0.392	383-473	0.53
x=0.1	0.044	313-383	0.365	383-473	0.82
x=0.3	0.062	313-413	0.367	413-473	0.94
x=0.5	0.091	313-413	0.373	413-473	1.10
x=0.7	0.100	313-413	0.349	413-473	1.71
x=0.9	0.144	313-413	0.306	413-473	3.85
CdO	0.045	313-413	0.261	413-473	4.09

The Hall effect properties were calculated for all samples to examine their charge carrier concentration and carrier mobility. The results shows that pure PbO and samples with low CdO contents (0.1 and 0.3), prepared by Pulsed Laser Deposition Technology, were P-type, while the high CdO content samples and pure CdO films were n-type. the results of ($PbO_{1-x}CdO_x$) thin films that prepared by different percentages, at room temperature, their increasing of percentage of cadmium oxide would increasing electrical conductivity and mobility.

Table (5) show the values of charge carriers concentration and mobility and electrical conductivity for the (PbO and CdO) films that prepared by different x percentages. We note from the table that the mobility increase with the increase of cadmium oxide ratio, that due to the increase in average of grain size and low grain boundary density.

Table 5 : charge carrier concentration, mobility and conductivity at RT for PbO_{1-x} CdO_x thin films at different x ratio

X	σ_{RT} ($\Omega^{-1}.cm^{-1}$)	R_H	$n\times10^{15}$ (cm^{-3})	type	μ_H (cm^2/v.sec)
0.0	1.99E-05	928500	0.007	P	18.44
0.1	2.10E-05	2321000	0.003	p	48.65
0.3	2.03E-05	1012000	0.006	p	20.49
0.5	2.00E-05	-1155000	0.005	n	23.13
0.7	3.55E-04	-1880.0	3.324	n	0.67
0.9	1.74E-01	-857.3	7.290	n	149.43
1.0	1.10E+01	-69.7	89.644	n	769.71

Conclusion

Thin film (PbO:CdO) and their composite, with different ratio, thin films were successfully deposited by PLD technique, these thin films have a variety in their structural, optical and electrical properties depending on the ratio. The X- ray diffraction measurement shows that all films have polycrystalline structure. . The pure PbO sample has many peaks corresponding to three phase, Tetragonal PbO, Orthorhombic PbO and Tetragonal Pb_3O_4, with preferred orientation along (011) Tetragonal PbO. There are some peaks correspond to Hexagonal Cd phase at the (0.3 ,0.5) ratio, also new peaks corresponding to Cubic $CdPbO_3$ phase at the (0.7) ratio. These patterns shows that increase the CdO ratio cause to appear of new peaks corresponding to CdO and, while the decreasing in PbO peaks intensities till finished at the (0.9) ratio and only CdO peaks appeared. AFM measurements show that the all film are uniformly distributed over the surface. The gran size increase with increasing the ratio.
UV-Visible measurements show that the absorption decrease with increasing CdO ratio from 3.5 to 0.7 at 600 nm, while the energy gap increase from 2.6 to 2.9 eV with it.
Electrical properties show enhance the films conductivity with increasing CdO ratio and convert from P-type to n-type at 0.5 PbO:CdO thin films ratio.

References

M.H.Madhusdhan Reddy, S.R.Jawalekar and A.N.Chandorkar, Thin Solid Films, 117-169 (1989).

M. Martín "TeO2-based film glasses for photonic applications: structural and optical propertie " Madrid, septiembre (2009).

M. Suganya, V. Narasimman, J. Srivind, "Studies On The Physical Properties Of Spray And Silar Deposited Lead Oxide Thin Films", Journal of Electron Devices, Vol. 21, pp. 1842-1848, (2015).

P. A. Radi, A. G. Brito-Madurro, J. M. Madurro, and N. O. Dantas, "Characterization and Properties of CdO Nanocrystals Incorporated in Polyacrylamide", Brazilian Journal

of Physics, vol. 36, no. 2A, June, (2006).

W. H. Bragg and W. L. Bragg, X Rays and Crystal Structure. London: G. Bell and Sons, LTD., 1918.

P. Yang, The Chemistry of Nano Structured Materials. Printed in Singapore.: World Scientific Publishing Co. Pte. Ltd., p. 362, 2003.

Garcia ,R. and R. Perez ,“ Dynamic atomic force microscopy methods ”, Surface science reports, Vol. 47, p.p. 197-301, (2002).

S. Elliott, "Physics of Amorphous Materials", Longman Inc., New York, Vol. 155, (1984), P.98.

H.K. Pulker, “Characterization of optical thin films,” Applied Optics, 18 (1979) P.1969.

P. S. Kireev, *Semiconductors physics*, 2nd editio. translated from the Russian by M. Samokhvalov, Mir puplishers Moscow, 1978.